HHS Public Access

Author manuscript

Cancer. Author manuscript; available in PMC 2018 May 15.

Published in final edited form as:

Cancer. 2017 May 15; 123(6): 1051–1060. doi:10.1002/cncr.30419.

Intraoperative Near-Infrared Fluorescence Imaging Targeting Folate Receptors Identifies Lung Cancer in a Large Animal Model

Jane Keating, MD[1,2], **Jeffrey Runge, DVM**[2,3], **Sunil Singhal, MD**[1,2], **Sarah Nims, BS**[1,2], **Ollin Venegas, BA**[1,2], **Amy Durham, VMD**[4], **Gary Swain, PhD**[4], **Shuming Nie, PhD**[5], **Philip Low, PhD**[6], and **David Holt, BVSc**[2,3]

[1]Department of Surgery, University of Pennsylvania Perelman School of Medicine, Philadelphia, PA

[2]Center for Precision Surgery, Abramson Cancer Center, University of Pennsylvania Perelman School of Medicine, Philadelphia, PA

[3]Department of Clinical Studies, University of Pennsylvania School of Veterinary Medicine, Philadelphia, PA

[4]Department of Pathobiology, University of Pennsylvania School of Veterinary Medicine, Philadelphia, PA

[5]Departments of Biomedical Engineering and Chemistry, Emory University, Atlanta, GA

[6]Department of Chemistry, Purdue University, West Lafayette, IN

Abstract

Background—Complete tumor resection is the most important predictor of patient survival from non-small cell lung cancer. Methods of intraoperative margin assessment following lung cancer excision are lacking. We evaluated near-infrared intraoperative imaging using a folate-targeted molecular contrast agent (OTL0038) for localization of primary lung adenocarcinoma, lymph node sampling, and margin assessment.

Methods—Ten dogs with lung cancer underwent either video-assisted thoracoscopic surgery (VATS) or open thoracotomy and tumor excision following intravenous injection OTL0038. Lungs were imaged using a NIR imaging device both *in vivo* and *ex vivo*. The wound bed was re-imaged for retained fluorescence suspicious for positive tumor margins. Tumor signal-to-background ratio (SBR) was measured in all cases. Next, three human patients were enrolled in a proof-of-principle study. Tumor fluorescence was measured both *in situ* and *ex vivo*.

*Corresponding Author: Jane Keating, MD, janejkeating@gmail.com.

Author Contributions: JK wrote the majority of the manuscript. JR and DH performed the canine operations. DH also wrote a substantial portion of the manuscript and was the primary editor. SN, JK and OV assisted in intraoperative imaging, patient coordination and post-operative image quantification. AD and GS provided the pathological correlation of each tumor specimen. SN and PL were the primary developers of OTL0038 and provided guidance for dosing and imaging decisions. SS performed the human operations and edited the manuscript.

Conflict of Interest: There are no conflict of interest disclosures for any author other than Dr. Low. Dr. Low reports grants and personal fees from On Target Laboratories. In addition, Dr. Low has a patent On Target Laboratories licensed.

Results—All canine tumors fluoresced *in situ* (Fluoptics mean SBR 5.2 (range 2.7-8.1); Karl Storz mean SBR 2.9 (range 1.4-2.6). Additionally, fluorescence was consistent with tumor margins on pathology. Three positive lymph nodes were discovered using NIR imaging. Also, a positive retained tumor margin was discovered upon NIR imaging of the wound bed. Human pulmonary adenocarcinomas were also fluorescent both *in situ* and *ex vivo* (mean SBR > 2.0).

Conclusions—NIR imaging identifies lung cancer in a large animal model. Additionally, NIR imaging can discriminate lymph nodes harboring cancer cells and also bring attention to a positive tumor margin. In humans, pulmonary adenocarcinomas fluoresce after injecting the targeted contrast agent.

Keywords

Lung cancer; imaging; molecular; near-infrared; intraoperative

Introduction

Lung cancer is the leading cause of cancer-related death in the United States with an estimated mortality of 164,000 patients in 2014[1]. Surgical resection is the mainstay of treatment for patients with stage I, II, and a subset of those with stage IIIA non-small cell lung cancer (NSCLC)[2, 3]. The most important predictors for patient survival are accurate staging and complete surgical resection. Specifically, patients with complete surgical resection have significantly better survival compared to those with partial or incomplete resection[4-8].

Surgical precision depends on complete tumor removal with disease-free margins and identification of regional metastatic disease. The visual information, tactile cues, and experience used by surgeons to identify a tumor and surgical margins are subjective and may lead to erroneous decisions. Currently, there are minimal intraoperative techniques for margin detection for lung cancer. One technique, frozen section, is costly, time-consuming, and requires a specialized pathologist[9]. Therefore, there is a need for reliable, objective, real-time imaging during surgery to delineate a tumor from normal tissue and evaluate regional lymph nodes and local structures for metastatic disease.

Intraoperative molecular imaging provides objective, real-time visualization of tumors during surgery allowing for accurate resection of the tumor and adequate margins of normal tissue. Different approaches to fluorescence imaging, including various optical contrast agents, antibody conjugates, peptide conjugates, and tumor-activated probes have been investigated. The potential utility of intra-operative fluorescence-guided tumor resection has been evaluated in pre-clinical studies and in a limited number of patients with breast, ovarian, pancreatic and hepatic cancers, gliomas, and non-small cell lung cancers[10-18]. We have shown that near-infrared (NIR) fluorescence imaging using indocyanine green (ICG) can identify lung tumors and other solid tumors including breast cancer and thymomas in canine and human patients[12, 14, 15, 19, 20]. ICG is thought to accumulate in tumors through leaky tumor vasculature and decreased lymphatic drainage (the “enhanced permeability and retention” effect), which is effective but non-specific[21-23].

Our group has had success using a folate-targeted visible spectrum optical contrast agent, folate-FITC, for the localization and margin assessment of pulmonary adenocarcinomas and ovarian cancer and metastasis[24-26]. Folate receptor alpha is highly expressed on several cancer types including ovarian cancer, colorectal cancer and >80% of pulmonary adenocarcinomas. It therefore provides a reliable target for optical contrast agents. Folate-FITC has an excitation wavelength of 495 nm and emits at 520 nm. Although successful, our studies using folate-FITC were limited by autofluorescence from surrounding normal tissue and a lack of depth of penetration into the lung. Molecularly targeted dyes, fluorescing in the near-infrared spectrum, as opposed to visible spectrum agents, have the potential to overcome these challenges.

We hypothesized that a novel folate receptor targeted NIR dye would identify lung tumors during surgery in a pilot study using spontaneously occurring canine primary lung tumors that provides an excellent large animal model of human non-small cell lung cancer in humans. First, we showed the NIR folate receptor-targeted dye can localize to lung tumors and lymph nodes, and then we demonstrated that retained fluorescence provides information regarding tumor margins. Lastly, we performed a proof-of-principle study of NIR intraoperative molecular imaging in three human patients with preoperatively diagnosed pulmonary adenocarcinoma.

Materials and Methods

Folate receptor-targeted contrast agent

A NIR folate receptor (FR)-targeted contrast agent was produced at clinical grade according to GMP conditions by On Target Laboratories, LLC and then supplied on a non-GMP basis to the University of Pennsylvania School of Veterinary Medicine. The contrast agent, known as OTL0038, is a folate analog ligand conjugated with an indole cyanine-like green dye. OTL0038 excites at 774-775 nm and emits at 794-796 nm. The agent targets folate receptor and is internalized into the cytoplasm. All vials of OTL0038 were supplied after approval of the Investigational Medicinal Product Dossier documentation according to US Food and Drug Administration (FDA). The imaging agent was stored, recorded and monitored before release by the Hospital Pharmacy according to FDA and Good Clinical Practice (GCP) guidelines. OTL0038 was dissolved in phosphate buffered saline and injected intravenously at a dose of 0.185 mg/kg over a period of 5 minutes 2-3 hours before surgery.

Our dose of 0.185 mg/kg of intravenous OTL0038 was based on preclinical small-animal studies performed in our lab. In these studies, which have not yet been published, we found that optimal tumor imaging occurred with intravenous injection and imaging performed 2-3 hours following infusion. This was the lowest dose and optimal timing in which tumor fluorescence was brightest when compared to background fluorescence. Additionally, we found no evidence of animal toxicity from OTL0038 infusion or imaging. In a separate and currently ongoing phase I clinical trial, our preliminary data shows no toxicity in patients except for one instance of a grade one hypersensitivity reaction consisting of a minor rash which resolved with an antihistamine and discontinuation of drug infusion. Likewise, the structure of OTL0038 is similar to indocyanine green (ICG). ICG has been well tolerated for decades with a favorable safety profile and is primarily used for perfusion imaging.

Imaging Systems

Fluorescence imaging was performed in 4 cases with a commercial NIR imaging system (Fluobeam ™, Fluoptics, Grenoble, France). NIR excitation light was generated by a laser emitting at 785 nm. The laser illuminated a 6cm diameter area at a 17cm working distance. The optical head contained a sensitive charged-coupled device camera allowing visualization of NIR fluorescence in the surgical field.

A NIR-optimized thoracoscopic system was used in 6 cases (Karl Storz GmbH & Co. KG Tuttlingen, Germany). Light was generated by xenon light source (20133701-1, D-light P, Karl Storz) that included an integrated filter turret permitting the user to switch appropriate filters into the light transmission pathway. The specially designed dichroic filter set enabled excitation of OTL0038 fluorescence at its $\lambda_{absorption}$ maxima in parallel with back ground illumination of the surgical field. Switching the filter out of the pathway permitted standard white light observation. OTL0038 fluorescence was visualized using a high definition, NIR-imaging, three-chip charged coupled device camera (22220085-3 H3-Z FI camera head; 22201011-112, IMAGE 1 HUB™ camera control unit, Karl Storz) coupled to a 30° 10 mm Hopkins® Forward-Oblique telescope (26003 BGA, Karl Storz). The telescope transmits light in the OTL0038 $\lambda_{emission}$ maxima range.

Canine subjects

Between April and November 2014, 10 dogs with primary lung tumors that were deemed surgical candidates were recruited from the University of Pennsylvania School of Veterinary Medicine. The canine study was approved by the University's Institutional Animal Care and Use Committee. The consent document was approved by the Veterinary School's Privately Owned Animal Protocol Committee and written informed consent was obtained from all owners.

The imaging systems were used to inspect the surgical field before and after the pulmonary resection. Fluorescence readings were taken from the tumor and grossly normal lung in the affected lobe. The tumor periphery was imaged in 4 radial directions (12, 3, 6, and 9 o'clock positions). Grossly normal lung 5mm and 10mm extending away from the tumor periphery was then imaged where possible and was used as background readings. Following lobectomy, the hilus of the lobe and any visible bronchial lymph nodes were imaged in NIR, and excised specimens were imaged *ex vivo* prior to submitting them for histopathological evaluation. The tumor margins were determined by fluorescence and marked with suture and were subsequently compared with histopathological margins.

Immunohistochemistry

Formalin-fixed paraffin-embedded tissue sections were washed in xylene (2×7') followed by ethanol (100% 2×4'; 95% 2×1' and 70% 1×1') prior to antigen retrieval with Citra solution (HK086-9K, Biogenex, Freemont, CA). The sections were boiled and then sat for 25 minutes in the hot buffer. Endogenous peroxidases were quenched with 3% hydrogen peroxide for 15 minutes and washed. Biotin was blocked using an avidin-biotin blocking kit according to manufacturers instructions (SP-2001, Vector labs, Burlingame, CA). Protein

blocking was done at room temperature for 15 minutes (Starting Block T20 37539, Thermo Scientific, Rockford IL).

The primary antibody, rabbit anti FOLR1 / Folate Receptor Alpha (LSBio #LS-B5727) was diluted 1:750 in Antibody Diluent (003118, Life Technologies, Fredrick, MD) and applied to the sections for 60 minutes at 37 degrees. The slides were then washed in PBS (2×5') and a biotinylated anti-rabbit secondary (BA-1000 Vector labs, Burlingame, CA) was applied for 30 minutes at 37 degrees. Following PBS washes (2×5') avidin-biotin-complex reagent (VectaStain Elite PK-6100, Vector labs, Burlingame, CA) was applied for 30 minutes at 37 degrees. Slides were washed 2×5' in PBS and signal was developed using a DAB reagent kit (SK-4100, Vector labs, Burlingame, CA). Slides were counterstained with hematoxylin, dehydrated through ethanols, cleared in xylene and mounted with Cytoseal XYL (8312-4, Thermo Scientific, Rockford IL).

Quantification of signal-to-background ratios

The fluorescence of tumor and normal lung *in situ* and *ex vivo* was evaluated using the region of interest (ROI) plugin of ImageJ® and compared as signal-to-background ratios (SBR). The range, mean, and standard deviation of fluorescence intensity within each specific region of interest were obtained using the ImageJ® histogram function. The "signal" was quantified as the average fluorescence from the regions identified as tumor. The "background" was identified as the average fluorescence of normal lung tissue. Fluorescence of the tumor margins in the four radial directions was compared to fluorescence of normal lung tissue immediately adjacent to the tumor in those locations where applicable. Fluorescence of identified lymph nodes was compared to either normal lymph node tissue (subsequently confirmed by histopathology) or the highest fluorescence value for normal tissue in that dog. Mean fluorescence values from tumor and normal lung and tumor-positive and tumor-negative lymph nodes were compared using two tailed t tests. Statistical analyses were performed in Stata Version 12.1 (StataCorp, College Station, TX).

Human Trial

Between March and June 2015, three patients with diagnosed pulmonary adenocarcinoma were enrolled in a proof-of-principle study. The study was approved by the University of Pennsylvania Institutional Review Board, and all patients gave informed consent. Patients underwent computed tomography scanning with 1 mm slice thickness that was reviewed by a radiologist to confirm the presence of a pulmonary nodule. Subsequently, each patient underwent transthoracic or transbronchial biopsy demonstrating cancer cells prior to enrollment.

Surgeons performed typical VATS and located the lung nodule using thoracoscopy, finger palpation, and NIR fluorescence. All NIR imaging was performed using the Karl Storz thoracoscopic system.

Following NIR imaging, the specimen was re-imaged on the back table before submitting to pathology.

Results

NIR Intraoperative Fluorescence Imaging Identifies Pulmonary Adenocarcinoma *In Situ*

Ten dogs were enrolled in the study. Ages ranged from 7 to 13 years (Median 11 years) and weights ranged from 3.8-37.0 kg (Median 13.0 kg). The OTL0038 infusions were well tolerated and no adverse reactions were observed. Six dogs had pulmonary carcinomas and four had adenocarcinomas that were confirmed with preoperative biopsy. Mean tumor size was 6.1 cm (Range 3.0 cm-10.0 cm). Canine characteristics are summarized in Table 1.

Four dogs underwent open thoracotomy and were imaged with the Fluoptics system and six underwent VATS excision and were imaged with the Karl Storz NIR endoscopic system. NIR fluorescent imaging clearly identified the tumor in all cases. Mean tumor fluorescence averaged from all four quadrants of the tumor was 33,390 A.U. (Range 9,524 A.U.-52,415 A.U.) using the Fluoptics system and 42.8 A.U. (Range 26.5 A.U.-50.5 A.U.) using the Karl Storz system. Mean background fluorescence using the Fluoptics system was 3,478 A.U. (Range 616 A.U.-6,352 A.U.) and using the Karl Storz was 21.1 (Range 16.0 A.U.-26.5 A.U.) (Fig. 1). Tumor fluorescence was significantly higher than fluorescence from normal lung in all cases with either imaging system ($p<0.001$; Mean SBR 5.2 (Fluoptics range = 2.7-8.1)); mean SBR 1.9 (Karl Storz range = 1.4-2.6)).

NIR Fluorescence Imaging Identifies Tumor Margins *Ex Vivo*

Following tumor resection, each specimen was re-imaged on the back table using the NIR imaging device in order to assess the presence of fluorescence at the margins. Macroscopic tumor margins were measured for fluorescence in all 4 radial directions. In all cases, the macroscopic tumor margins were fluorescent, with a mean margin fluorescence of 24,502 A.U. (18, 519 A.U.-37,817 A.U.) using the Fluoptics system and 71.5 A.U. (66.2 A.U.-77.0 A.U.) using the Karl Storz system. Next, background fluorescence in the normal lung was measured in the 4 radial directions as previously described. Complete values of background fluoresce readings were not available because of lack of adjacent normal lung in 1-3 quadrants in 6 specimens. The mean background fluorescence at 5mm was 5,934 A.U. (5,322 A.U.-6,599 A.U.) using the Fluoptics system and 42.6 A.U. (37.0 A.U.-46.3 A.U.) using the Karl Storz system. Likewise, the mean background fluorescence at 10mm was 3,211 A.U. using the Fluoptics system and 26.8 A.U. using the Karl Storz system (Fig. 2).

A stitch was placed using fluorescence guidance at the macroscopic tumor border and in the normal lung in all radial directions prior to submission to pathology. Pathology confirmed tumor presence at the areas of fluorescence and normal lung at the location of background fluorescence. Additionally, IHC confirmed 2+ or 3+ FR staining in all tumor specimens.

NIR Fluorescence Imaging Identifies Positive Lymph Nodes

Following tumor excision, the specimen was re-imaged for evidence of lymph nodes using both traditional white light and the NIR imaging device. As per standard of care for canine subjects, no significant dissection was performed in order to search for lymph nodes. However, in three cases, NIR imaging using the Fluoptics imaging device identified markedly fluorescent regional bronchial lymph nodes (SBRs = 2, 4.3, and 5 respectively;

p<0.001 in all cases), and they were sent for pathological correlation (Fig. 3). All three fluorescent lymph nodes were found to be metastatic for tumor cells by a board certified veterinarian pathologist.

Likewise, one additional lymph node was found using traditional white light imaging. In this case, the lymph node was also imaged using the NIR imaging device. However, unlike the previously described three nodes, this bronchial lymph node did not fluoresce either compared to normal tissue. Following excision and biopsy, this lymph node was tumor negative on H&E.

The fluorescent lymph nodes were stained using immunohistochemistry and were found to be 3+ FR positive in all cases. In the case of the non-fluorescent lymph node, which was found to be negative for tumor metastasis, IHC found weakly positive (1+) staining.

NIR Fluorescence Imaging Identifies A Positive Tumor Margin

Following tumor resection, NIR imaging was used to reimage the wound bed in order to look for residual fluorescence concerning for retained tumor. In 9 out of 10 cases, no fluorescence was noted in the wound bed (mean SBR <1.2). In all 9 instances, the resected specimen was noted to have widely negative margins (tumor located >1 cm from margin).

However, in one case, fluorescence was noted on the hilum during both *ex vivo* and wound bed imaging. This case is detailed here: Buckwheat is an 11-year-old laborador retriever. He presented for coughing to the surgeon (DH). He was found to have a 5 cm biopsy proven pulmonary adenocarcinoma in his right caudal lobe. He was consented for surgery and tolerated OTL0038 infusion 2.5 hours prior to surgery. He underwent imaging with the Karl Storz thoracoscopic imaging system. His tumor was fluorescent with an *in vivo* SBR of 1.4. Following specimen excision and imaging, the wound bed was reimaged which demonstrated an area of retained fluorescence in the bronchus (SBR = 1.8 compared to adjacent normal bronchus; $P < 0.001$) (Fig. 4). This additional fluorescent bronchial tissue was removed. Biopsy and H&E of this tissue confirmed foci of carcinoma at the resected bronchial margin.

Canine Outcomes

All dogs survived the perioperative period and were discharged from the hospital. The three dogs with tumor positive lymph nodes survived less than 4 months (Range = 1-3 months). The dog with the fluorescent wound bed and corresponding tumor positive margin is alive 9 months after surgery but has evidence of tumor recurrence on follow-up thoracic radiographs obtained with his local veterinarian. All remaining dogs are alive more than 12 months after surgery and show no clinical evidence of cancer recurrence.

OTL0038 Localizes to Pulmonary Adenocarcinoma in Humans

Following the success of our animal study, we enrolled three human patients with preoperatively diagnosed pulmonary adenocarcinoma in a proof-of-principle clinical trial. All patients underwent NIR imaging using the Karl Storz thoracoscope. All tumors were found to be fluorescent *in vivo* (mean SBR 2.8 (range 2.2-3.4)) and *ex vivo* (mean SBR 3.3

(range 2.8-3.7). One patient example is discussed here: DR is a 55-year-old female with a 45 pack-year smoking history. She presented to her primary care physician with an incidental pulmonary nodule located in the left lower lobe noted on CT scan. She underwent transthoracic needle biopsy and was diagnosed with pulmonary adenocarcinoma. She underwent OTL0038 injection of 0.025 mg/kg via antecubital vein 3 hours prior to imaging with no adverse events.

Following traditional localization, the Karl Storz NIR thoracoscope was turned on. The pulmonary nodule was noted to be fluorescent with an *in situ* SBR of 3.4 (Fig. 5). The nodule was excised via wedge resection and was fluorescent on the back table, and there was no fluorescence noted at the staple line. Upon reimaging of the wound bed, no additional fluorescence was seen which would have indicated disease left behind. Final pathology confirmed a 3.5 cm pulmonary adenocarcinoma with negative margins. All patient demographics and tumor characteristics are summarized in table 2. One patient with stage II disease underwent postoperative chemotherapy. No patient has evidence of recurrent cancer with an average follow up time of 5.7 months (range 4-7 months).

Discussion

Intraoperative margin assessment of solid tumors is important for complete resection, clinical staging, and postoperative planning. Different approaches to improve intra-operative lung tumor margin assessment are utilized with various successes. For example, frozen sections of representative tumor margins can be evaluated by pathologists during surgery. However, evaluation of an entire margin would require thousands of sections, which is impractical[27]. Other methods of tumor detection include ultrasound, which is unlikely to identify small residual tumor foci, and radiofrequency spectroscopy, which is not easily adaptable to the clinical surgery setting[28, 29]. The limitations of margin assessment modalities have led our group to investigate real-time tumor imaging using a variety of fluorescent probes and imaging systems.

Spontaneous canine lung cancer occurs in animals with owners who smoke tobacco and are most often adenocarinomas. In this study, intraoperative molecular imaging using a NIR folate-targeted fluorescent agent and two NIR imaging devices identified canine lung tumors and their margins in all canine and human cases. Additionally, OTL0038 also identified three tumor-positive regional lymph nodes and one tumor-positive surgical margin. These results illustrate the potential for NIR fluorescent imaging to accurately detect primary and regional pulmonary metastatic disease, which may allow for more complete resections.

As a NIR agent, OTL0038 fluorescent light has the added benefit of improved depth of penetration for imaging tumors deeper within the lung tissue when compared to visible spectrum agents like the previously described folate-FITC[30]. OTL0038 it is also a targeted agent, which should allow for improved depth of penetration and decreased local tissue autofluorescence and adenocarcinoma specific binding. Additionally, NIR imaging delivers 10^5 less energy than a chest radiograph, making it safe for patients[31].

We acknowledge several limitations in this study. Due to our relatively small sample size, we had one positive margin correlating with retained tumor bed fluorescence. Additionally, veterinary surgeons do not routinely visualize and remove all lymph nodes in surgery for canine lung cancer, and therefore we were only able to sample nodes which were obvious and easy to dissect. As such, we will rely on our human trial to investigate the implications of lymph node fluorescence.

Secondly, there is a need for the development of intraoperative fluorescence quantification. In this study, we have used postoperative fluorescence calculations using for measurement of signal to background ratio. Although this provides an accurate assessment of fluorescence, it does not provide quantitative data to the surgeon in real-time.

Intraoperative molecular imaging would be valuable to thoracic surgeons for the localization of small pulmonary tumors which are difficult to feel and see using traditional VATS. A fluorescent tumor would be easier to localize which may reduce both the need for conversion to open thoracotomy and operative time. Additionally, minimally invasive thorascopic techniques have become standard treatment for early stage non-small cell lung cancer in humans[32-36]. Importantly, the Karl Storz imaging device incorporates NIR imaging technology into a 30^0 10mm telescope. Likewise, although not used in this large animal study, robotic surgery may be carried out using the da Vinci ® Si ™ Surgical System equipped with Firefly technology which allows NIR imaging. This will be pertinent to research of this type in an upcoming human trial as robotic surgery increases in popularity[37-39].

The results of this study support the use of NIR thorascopic surgery with an appropriately targeted NIR contrast agent for the investigation of early stage non-small cell lung cancer to delineate tumor margins and identify metastatic lymph nodes. A clinical trail to validate these preliminary results is now underway

Acknowledgments

Funding: This work was supported by National Institutes of Health R0I CA193556 and R03 EB017828.

References

1. Siegel R, Naishadham D, Jemal A. Cancer statistics, 2013. CA Cancer J Clin. 63:11–30. [PubMed: 23335087]
2. Ramalingam SS, Owonikoko TK, Khuri FR. Lung cancer: New biological insights and recent therapeutic advances. CA Cancer J Clin. 2011; 61:91–112. [PubMed: 21303969]
3. Vallejo, Ocana C., Garrido, Lopez P., Muguruza, Trueba I. Multidisciplinary approach in stage III non-small-cell lung cancer: standard of care and open questions. Clin Transl Oncol. 2011; 13:629–635. [PubMed: 21865134]
4. Sienel W, Stremmel C, Kirschbaum A, et al. Frequency of local recurrence following segmentectomy of stage IA non-small cell lung cancer is influenced by segment localisation and width of resection margins--implications for patient selection for segmentectomy. Eur J Cardiothorac Surg. 2007; 31:522–527. discussion 527-528. [PubMed: 17229574]
5. Kaiser LR, Fleshner P, Keller S, Martini N. Significance of extramucosal residual tumor at the bronchial resection margin. Ann Thorac Surg. 1989; 47:265–269. [PubMed: 2537610]

6. Law MR, Hodson ME, Lennox SC. Implications of histologically reported residual tumour on the bronchial margin after resection for bronchial carcinoma. Thorax. 1982; 37:492–495. [PubMed: 7135287]
7. Snijder RJ, Brutel de la Riviere A, Elbers HJ, van den Bosch JM. Survival in resected stage I lung cancer with residual tumor at the bronchial resection margin. Ann Thorac Surg. 1998; 65:212–216. [PubMed: 9456120]
8. Soorae AS, Stevenson HM. Survival with residual tumor on the bronchial margin after resection for bronchogenic carcinoma. J Thorac Cardiovasc Surg. 1979; 78:175–180. [PubMed: 459524]
9. Marchevsky AM, Changsri C, Gupta I, Fuller C, Houck W, McKenna RJ Jr. Frozen section diagnoses of small pulmonary nodules: accuracy and clinical implications. Ann Thorac Surg. 2004; 78:1755–1759. [PubMed: 15511468]
10. Polom K, Murawa D, Rho YS, Nowaczyk P, Hunerbein M, Murawa P. Current trends and emerging future of indocyanine green usage in surgery and oncology: a literature review. Cancer. 2011; 117:4812–4822. [PubMed: 21484779]
11. Mohs AM, Mancini MC, Singhal S, et al. Hand-held spectroscopic device for in vivo and intraoperative tumor detection: contrast enhancement, detection sensitivity, and tissue penetration. Anal Chem. 2010; 82:9058–9065. [PubMed: 20925393]
12. Keating JJ, Kennedy GT, Singhal S. Identification of a subcentimeter pulmonary adenocarcinoma using intraoperative near-infrared imaging during video-assisted thoracoscopic surgery. J Thorac Cardiovasc Surg. 2015; 149:e51–53. [PubMed: 25827389]
13. Tagaya N, Yamazaki R, Nakagawa A, et al. Intraoperative identification of sentinel lymph nodes by near-infrared fluorescence imaging in patients with breast cancer. Am J Surg. 2008; 195:850–853. [PubMed: 18353274]
14. Holt D, Okusanya O, Judy R, et al. Intraoperative near-infrared imaging can distinguish cancer from normal tissue but not inflammation. PLoS One. 2014; 9:e103342. [PubMed: 25072388]
15. Okusanya OT, Holt D, Heitjan D, et al. Intraoperative near-infrared imaging can identify pulmonary nodules. Ann Thorac Surg. 2014; 98:1223–1230. [PubMed: 25106680]
16. van Dam GM, Themelis G, Crane LM, et al. Intraoperative tumor-specific fluorescence imaging in ovarian cancer by folate receptor-alpha targeting: first in-human results. Nat Med. 2011; 17:1315–1319. [PubMed: 21926976]
17. Gotoh K, Yamada T, Ishikawa O, et al. A novel image-guided surgery of hepatocellular carcinoma by indocyanine green fluorescence imaging navigation. J Surg Oncol. 2009; 100:75–79. [PubMed: 19301311]
18. Kovar JL, Simpson MA, Schutz-Geschwender A, Olive DM. A systematic approach to the development of fluorescent contrast agents for optical imaging of mouse cancer models. Anal Biochem. 2007; 367:1–12. [PubMed: 17521598]
19. Keating JJ, Nims S, Venegas O, et al. Intraoperative imaging identifies thymoma margins following neoadjuvant chemotherapy. Oncotarget. 2015
20. Keating J, Tchou J, Okusanya O, et al. Identification of breast cancer margins using intraoperative near-infrared imaging. J Surg Oncol. 2016
21. Prabhakar U, Maeda H, Jain RK, et al. Challenges and key considerations of the enhanced permeability and retention effect for nanomedicine drug delivery in oncology. Cancer Res. 2013; 73:2412–2417. [PubMed: 23423979]
22. Heneweer C, Holland JP, Divilov V, Carlin S, Lewis JS. Magnitude of enhanced permeability and retention effect in tumors with different phenotypes: 89Zr-albumin as a model system. J Nucl Med. 2011; 52:625–633. [PubMed: 21421727]
23. Matsumura Y, Maeda H. A new concept for macromolecular therapeutics in cancer chemotherapy: mechanism of tumoritropic accumulation of proteins and the antitumor agent smancs. Cancer Res. 1986; 46:6387–6392. [PubMed: 2946403]
24. Keating JJ, Okusanya OT, De Jesus E, et al. Intraoperative Molecular Imaging of Lung Adenocarcinoma Can Identify Residual Tumor Cells at the Surgical Margins. Mol Imaging Biol. 2015

25. Kennedy GT, Okusanya OT, Keating JJ, et al. The Optical Biopsy: A Novel Technique for Rapid Intraoperative Diagnosis of Primary Pulmonary Adenocarcinomas. Ann Surg. 2015; 262:602–609. [PubMed: 26366539]
26. Okusanya OT, DeJesus EM, Jiang JX, et al. Intraoperative molecular imaging can identify lung adenocarcinomas during pulmonary resection. J Thorac Cardiovasc Surg. 2015; 150:28–35. e21. [PubMed: 26126457]
27. Carter D. Margins of "lumpectomy" for breast cancer. Hum Pathol. 1986; 17:330–332. [PubMed: 3957334]
28. Allweis TM, Kaufman Z, Lelcuk S, et al. A prospective, randomized, controlled, multicenter study of a real-time, intraoperative probe for positive margin detection in breast-conserving surgery. Am J Surg. 2008; 196:483–489. [PubMed: 18809049]
29. Haid A, Knauer M, Dunzinger S, et al. Intra-operative sonography: a valuable aid during breast-conserving surgery for occult breast cancer. Ann Surg Oncol. 2007; 14:3090–3101. [PubMed: 17593330]
30. Pansare V, Hejazi S, Faenza W, Prud'homme RK. Review of Long-Wavelength Optical and NIR Imaging Materials: Contrast Agents, Fluorophores and Multifunctional Nano Carriers. Chem Mater. 2012; 24:812–827. [PubMed: 22919122]
31. Madajewski B, Judy BF, Mouchli A, et al. Intraoperative near-infrared imaging of surgical wounds after tumor resections can detect residual disease. Clin Cancer Res. 2012; 18:5741–5751. [PubMed: 22932668]
32. Flores RM, Park BJ, Dycoco J, et al. Lobectomy by video-assisted thoracic surgery (VATS) versus thoracotomy for lung cancer. J Thorac Cardiovasc Surg. 2009; 138:11–18. [PubMed: 19577048]
33. Farjah F, Wood DE, Mulligan MS, et al. Safety and efficacy of video-assisted versus conventional lung resection for lung cancer. J Thorac Cardiovasc Surg. 2009; 137:1415–1421. [PubMed: 19464458]
34. Whitson BA, Groth SS, Duval SJ, Swanson SJ, Maddaus MA. Surgery for early-stage non-small cell lung cancer: a systematic review of the video-assisted thoracoscopic surgery versus thoracotomy approaches to lobectomy. Ann Thorac Surg. 2008; 86:2008–2016. discussion 2016-2008. [PubMed: 19022040]
35. Yan TD, Black D, Bannon PG, McCaughan BC. Systematic review and meta-analysis of randomized and nonrandomized trials on safety and efficacy of video-assisted thoracic surgery lobectomy for early-stage non-small-cell lung cancer. J Clin Oncol. 2009; 27:2553–2562. [PubMed: 19289625]
36. Sugi K, Kaneda Y, Esato K. Video-assisted thoracoscopic lobectomy achieves a satisfactory long-term prognosis in patients with clinical stage IA lung cancer. World J Surg. 2000; 24:27–30. discussion 30-21. [PubMed: 10594199]
37. Ashitate Y, Tanaka E, Stockdale A, Choi HS, Frangioni JV. Near-infrared fluorescence imaging of thoracic duct anatomy and function in open surgery and video-assisted thoracic surgery. J Thorac Cardiovasc Surg. 2011; 142:31–38 e. 31–32. [PubMed: 21477818]
38. Oh Y, Lee YS, Quan YH, et al. Thoracoscopic color and fluorescence imaging system for sentinel lymph node mapping in porcine lung using indocyanine green-neomannosyl human serum albumin: intraoperative image-guided sentinel nodes navigation. Ann Surg Oncol. 2014; 21:1182–1188. [PubMed: 24310791]
39. Yamashita S, Tokuishi K, Anami K, et al. Video-assisted thoracoscopic indocyanine green fluorescence imaging system shows sentinel lymph nodes in non-small-cell lung cancer. J Thorac Cardiovasc Surg. 2011; 141:141–144. [PubMed: 20392454]

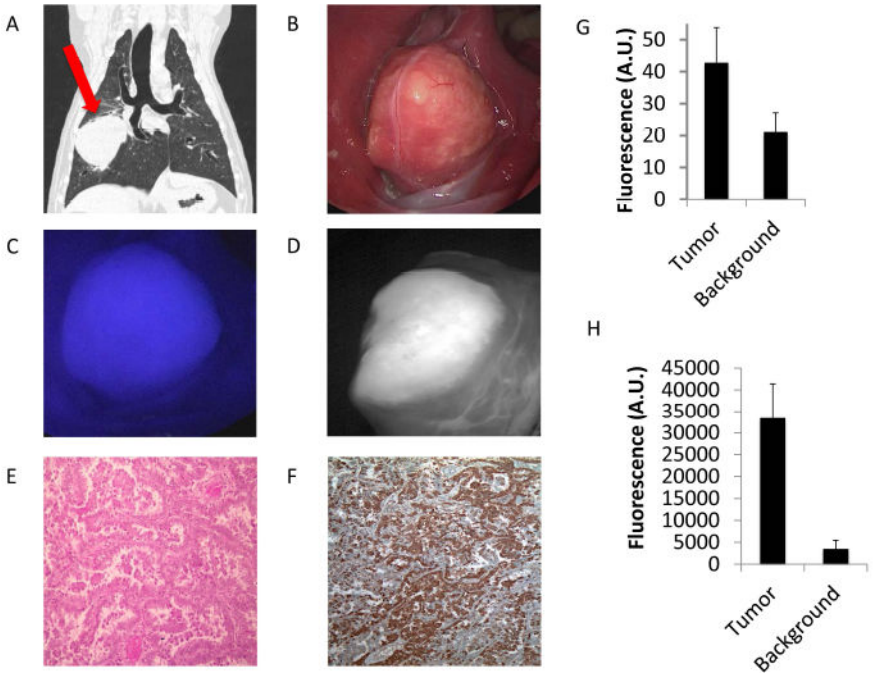

Figure 1.

A.) Preoperative CT scan showing an 8 cm right-sided pulmonary adenocarcinoma (red arrow). First the surgeon used B.) white light imaging *in vivo*. Next C.) the tumor is fluorescent *in vivo* with a SBR of 4.6 using the fluoptics and D.) was reimaged using the Karl Storz NIR camera confirming fluorescence. E.) H&E shows pulmonary adenocarcinoma and F.) IHC demonstrates 3+ FR staining. Next, graphic representation of the mean tumor and background fluorescence of tumors imaged using the G.) Karl Storz and H.) Fuloroptics NIR imaging is shown.

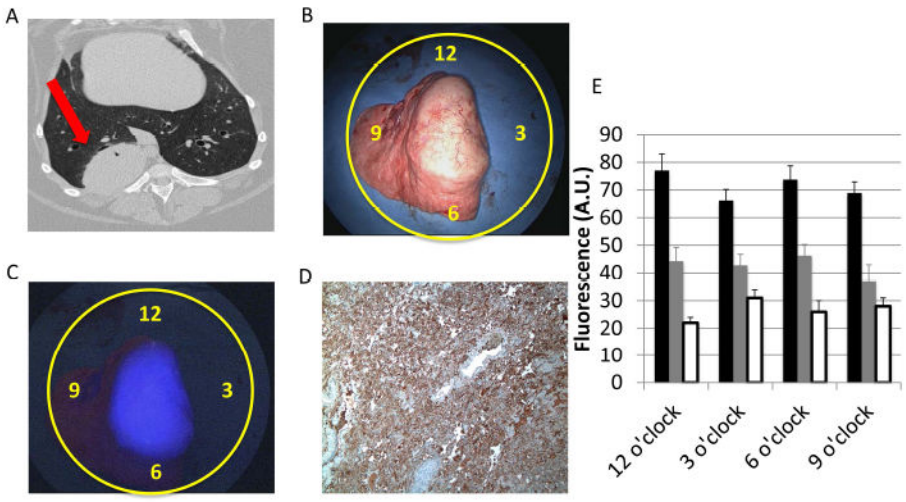

Figure 2.

A.) A preoperative CT scan showing a right-sided 5 cm lung tumor (red arrow). B.) A traditional white light *ex vivo* imaging of the specimen on the backtable. Yellow circles denote clock face and locations of both tumor margin and background fluorescence measurements. C.) NIR fluorescence image using the Karl Storz device. The tumor is circumscribed and brightly fluorescent with a mean SBR of 2.7. Note there was no available quantification of background fluorescence at 12 and 3 o'clock due to lack of surrounding normal lung. D.) Folate receptor IHC with 3+ FR tumor staining. E.) Fluorescence intensity decreases as distance from the tumor boarder increases. These measurements were obtained from tumors measured with the Karl Storz imaging system. The black bars represent tumor fluorescence directly at the tumor margin and the grey and white bars represent tumor fluorescence from the background (5 mm and 10 mm from the tumor edge, respectively).

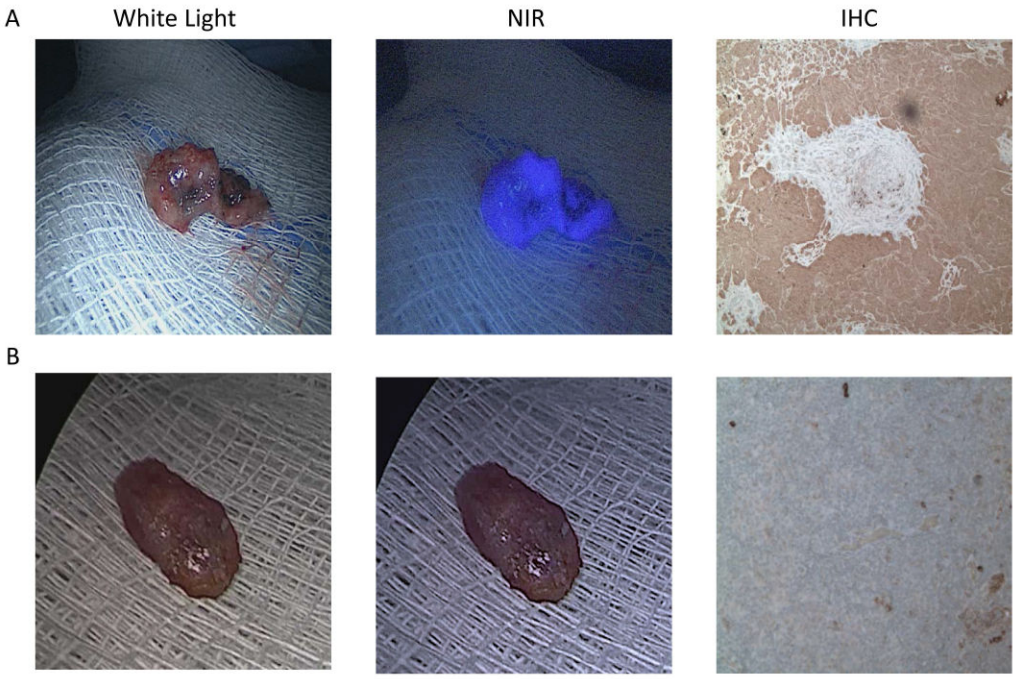

Figure 3.

Example images of *ex vivo* white light, *ex vivo* NIR, and FR IHC staining of a A.) cancer containing lymph node and B.) disease free lymph node.

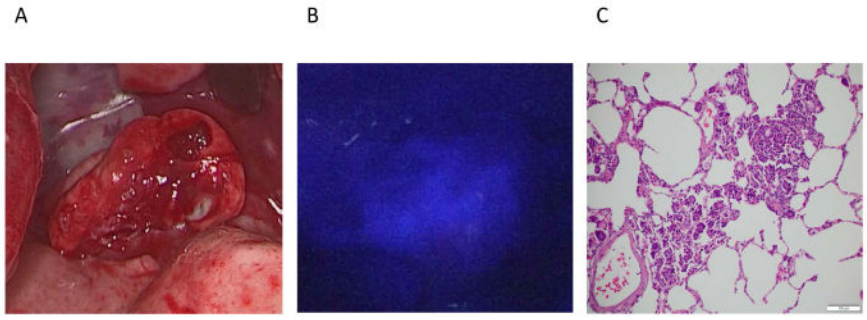

Figure 4.

Although not evident on traditional A.) white light imaging or palpation, one canine showed evidence of retained tumor cells using B.) NIR imaging of the wound bed following tumor excision. C.) Final pathology confirmed a positive margin at the bronchus.

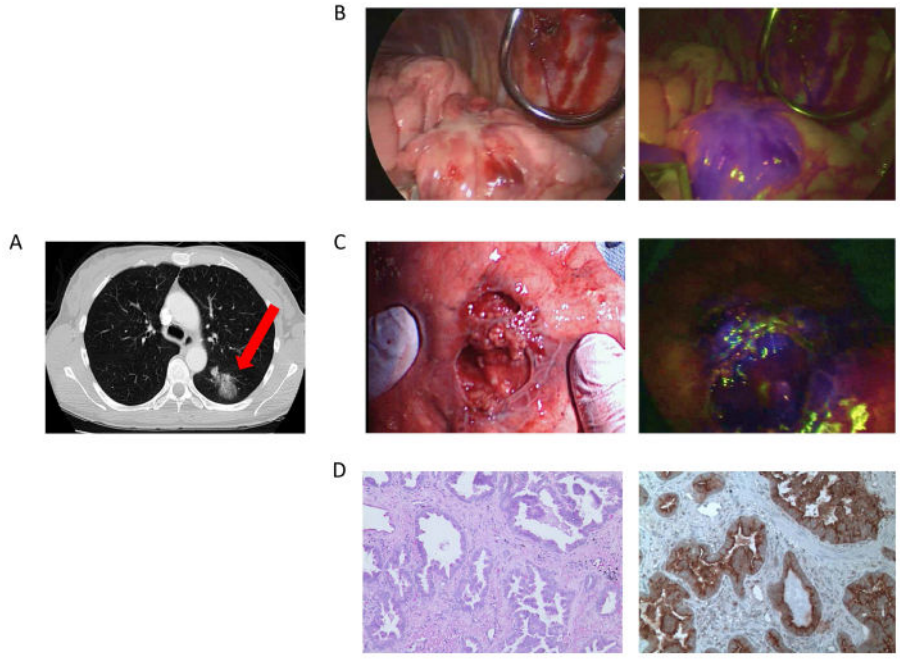

Figure 5.

Patient DR is a 55-year-old female with a mass in her left lower lobe noted on A.) preoperative CT scan which was confirmed pulmonary adenocarcinoma preoperatively. Images obtained intraoperatively include an B.) *in vivo* white light image, C.) NIR fluorescence image using the Karl Storz thoracoscopic system. Pathology confirmed D.) invasive adenocarcinoma on H&E. E.) IHC confirmed strong folate receptor staining.

Table 1

Canine demographics and tumor characteristics

Median age in years (range)	11 (7-13)
Sex	50% females
Mean tumor size in cm (range)	6.1 (3.0 – 10.0)
Canine breed	Mixed breed (N=2), Yorkshire Terrier (N=1), Miniature Pinscher (N=1), Cocker Spaniel (N=1), Rhodesian Ridgeback (N=1), Boxer (N=1), Samoyed (N=1), West Highland White Terrier (N=1), Labrador Retriever (N=1)
Involved hemithorax	
Right	N=4
Left	N=6
Tumor diagnosis	
Pulmonary adenocarcinoma	N =4
Pulmonary carcinoma	N=6
Surgical approach	
VATS	N=6
Thoracotomy	N=4

Table 2

Human demographics and tumor characteristics

Sex	2 females, 1 male
Age (years)	55, 62, 68
Tobacco smoking history (pack-years)	45, 42, 50
Tumor size (cm)	3.5, 5.2, 3.4
Involved hemithorax	2 right, 1 left
Surgical approach	All open thoracotomy
Tumor diagnosis	All pulmonary adenocarcinoma
Immunohistochemistry	FR 3+ in all cases
Tumor staging	Ia, IIa, Ib